

## Synthesis, Morphology, Spectral Characterization and Thermal Behaviors of Transition Metal Complexes Containing Oxime-Imine Group

Selma YILDIRIM UÇAN<sup>1\*</sup>, Hülya YILDIRIM<sup>2</sup>

<sup>1</sup>Department of Chemistry, Faculty of Arts and Sciences, Nigde Omer Halisdemir University, Nigde, Turkey

<sup>2</sup>Department of Mathematics and Science Education, Nigde Omer Halisdemir University, Nigde, Turkey

Geliş / Received: 03/09/2020, Kabul / Accepted: 07/12/2020

### Abstract

A new oxime-containing Schiff base ligand and its Cu(II), Ni(II), Zn(II) complexes have been synthesized. The structure of the ligand was identified by elemental analysis, UV-vis, FT-IR, <sup>1</sup>H NMR and <sup>13</sup>C NMR spectra. The synthesized complexes were characterized by FT-IR, SEM, TGA, elemental analysis, electronic spectra and magnetic susceptibility measurements. The Zinc(II) complex was also characterized by <sup>1</sup>H NMR spectra. Elemental analysis data of the metal complexes indicated that the metal: ligand ratio of the metal complex is 1:1. The magnetic susceptibility measurements and spectral data showed square-planar geometry for Cu(II) complex and tetrahedral geometry for Ni(II) complex.

**Keywords:** Oximes, Imines, Transition metal complexes, Thermal analysis, NMR chemical shifts

### Oksim-İmin Grubu İçeren Metal Komplekslerinin Sentezi, Morfolojisi, Spektral Karakterizasyonu ve Termal Davranışları

#### Öz

Yeni bir oksim içeren Schiff bazı ligandı ve onun Cu(II), Ni(II), Zn(II) kompleksleri sentezlendi. Ligandın yapısı element analizi, UV-vis, FT-IR, <sup>1</sup>H NMR and <sup>13</sup>C NMR spektrumları ile belirlendi. Sentezlenen kompleksler FT-IR, SEM, TGA, element analiz, elektronik spektrum ve manyetik duyarlılık ölçümleri ile karakterize edildi. Ayrıca çinko(II) kompleksi <sup>1</sup>H NMR spektrumu ile karakterize edildi. Metal komplekslerinin elementel analiz verileri, metal kompleksinin metal: ligand oranının 1: 1 olduğunu gösterdi. Manyetik süsseptibilite ölçümleri ve spektral veriler Cu (II) kompleksi için kare düzlem geometri ve Ni (II) kompleksi için tetrahedral geometri gösterdi.

**Anahtar Kelimeler:** Oksimler, İminler, Geçiş metal kompleksleri, Termal analiz, NMR kimyasal kaymaları

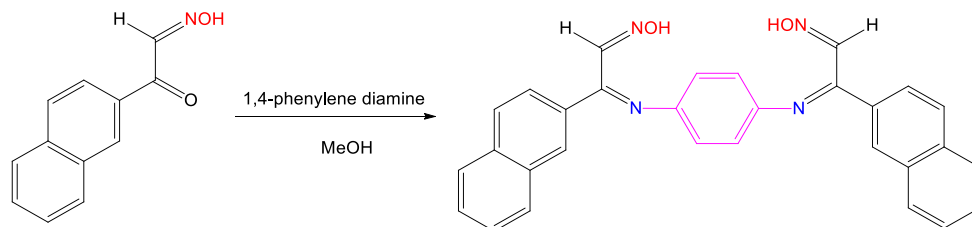
## 1. Introduction

Oximes and Schiff bases belong to a significant group of compounds. They are one of the most broadly used ligands because of the ease of formation and notable versatility and therefore they have played a substantial part in the improvement of inorganic compounds that composed steady complexes with 3d metals (Chakravorty, 1974; Dede et al., 2007; Tolga Çolak et al., 2009; Uçan and Mercimek, 2005). Diverse

3d complexes of the oxime-imine compound synthesized from the class of heterocyclic substances containing N and O has attracted much attention due to the simplistic structure. (Singh et al., 2007; Tadavi et al., 2018). 3d metal complexes of oximes-imines are reported to have a number of useful implementations in the analytical, clinical, biological and industrial fields (Radha et al., 2018; Al-Wabli et al., 2018; Dede et al.,

2018). However, this work describes the synthesis, characterization of nickel (II), zinc (II) and copper (II) complex obtained from the reaction of isonitroso-2-acetylnaphthalene and 1,4-phenylenediamine

(Scheme 1). The synthesized compounds were identified by elemental analysis, melting point, FT-IR, magnetic susceptibility, UV-Vis, SEM, thermal analysis,  $^1\text{H}$  NMR and  $^{13}\text{C}$  NMR.



**Scheme 1.** Preparation of 1,4-phenylimino-bis(isonitroso-2-acetylnaphthalene) (Ligand).

## 2. Material and Methods

### 2.1. Materials and Physical measurements

All chemicals and solvents utilized in the present work were of pure quality and were purchased from Sigma Aldrich. Isonitroso-2-acetylnaphthalene was synthesized according to our previous method (Yıldırım et al., 2003). Elemental analysis was conducted using a Carlo Erba 1106 instrument. Magnetic moment of three complexes was described to calibrate with  $\text{CuSO}_4$  by using Gouy balance at ambient temperature. A Varian T 200-A spectrometer was utilized to detect the NMR spectra in  $\text{DMSO}-d_6$  at ambient temperature. FT-IR spectra were enrolled with Pye Unicam instrument SP 1025 by forming potassium bromide pellet. UV-Vis. absorption spectra were measured using SHIMADZU 160 spectrophotometer in the range of 200-600 nm. The thermal analysis (DTA and TGA) were carried out by using a Shimadzu (TG-50 H model) thermal analyzer was started at room temperature to  $900^\circ\text{C}$  at a heating rate of  $10^\circ\text{C}/\text{min}$ . The SEM images of the complexes were analyzed by using ZEISS EVO 40.

### 2.2. Synthesis of Ligand

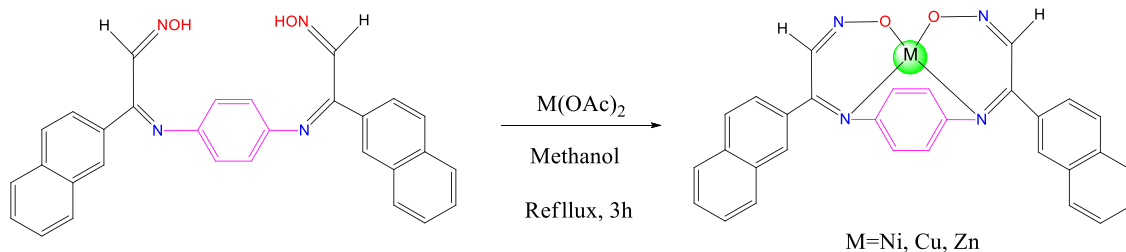
Isonitroso-2-acetylnaphthalene (3.900 g, 20 mmol) in methanol (30 mL) was stirred with a 1, 4-phenylene diamine (1 g, 10 mmol) in methanol (20 mL) for 5 h at  $28^\circ\text{C}$ . The orange colored solid obtained was filtered and then was washed with ethanol. The solid was recrystallized from dichloromethane and dried at  $40^\circ\text{C}$  over anhydrous calcium chloride in a vacuum. The purity of the product was controlled by TLC. Yield 82%, mp:  $159\text{--}161^\circ\text{C}$ . IR (KBr) spectrum,  $\text{v}/\text{cm}^{-1}$ :  $3260\text{w}$  (OH),  $3090\text{w}$  ( $\text{C}-\text{H}_{\text{arom}}$ ),  $1645\text{s}$  ( $\text{C}=\text{N}$ )<sub>imine</sub>,  $1620\text{s}$  ( $\text{C}=\text{N}$ )<sub>oxime</sub>,  $980\text{w}$  ( $\text{N}-\text{O}$ )<sub>oxime</sub>.  $^1\text{H}$  NMR spectrum ( $\text{DMSO}-d_6$ ),  $\delta$ :  $9.15$  (s, 2H, NOH)<sub>oxime group</sub>,  $8.80$  (s, 2H, HC=N)<sub>oxime</sub>,  $8.50\text{--}7.75$  (m, 18H,  $\text{C}-\text{H}_{\text{arom}}$ ). Elemental anal. (%) calcd. For  $\text{C}_{30}\text{H}_{22}\text{N}_4\text{O}_2$ : C 76.58; H 4.71; N 11.91; Found: C 76.44, H 4.55, N 11.71.

### 2.3. Synthesis of Complexes

1 mmol of the metal acetate solution [0.248 g  $\text{Ni}(\text{CH}_3\text{COO})_2 \cdot 4\text{H}_2\text{O}$ , 0.199 g  $\text{Cu}(\text{CH}_3\text{COO})_2 \cdot \text{H}_2\text{O}$  and 0.219 g  $\text{Zn}(\text{CH}_3\text{COO})_2 \cdot 2\text{H}_2\text{O}$ ] in 20.0 mL of EtOH was incorporated to 1 mmol (0.470g) of the

Schiff base solution in 40 mL of EtOH. The reaction was stirred under reflux for 3h at 65 °C. The product was filtered, washed with EtOH and then was dried at 40 °C over anhydrous calcium chloride in a vacuum. Nickel(II) Complex was obtained as a green powder (Scheme 2). Yield 74%, m.p. 208–210 °C. IR (KBr) spectrum,  $\nu/\text{cm}^{-1}$ : 3050w ( $\text{C-H}_{\text{arom}}$ ), 1620s ( $\text{C=N}_{\text{imine}}$ ), 1595s ( $\text{C=N}_{\text{oxime}}$ ), 975m ( $\text{N-O}_{\text{oxime}}$ ), 470w ( $\text{M-N}$ ), 420w ( $\text{M-O}$ ). Elemental anal. (%) calcd. For  $\text{C}_{30}\text{H}_{20}\text{N}_4\text{NiO}_2$ : C 68.35, H 3.82, N 10.63; Found: C 68.23, H 3.58, N 10.38. Copper(II) complex was obtained as a dark-green powder. Yield 77%, m.p. 147–148°C. IR (KBr) spectrum,  $\nu/\text{cm}^{-1}$ : 3045w ( $\text{C-H}_{\text{arom}}$ ),

1625s ( $\text{C=N}_{\text{imine}}$ ), 1600s ( $\text{C=N}_{\text{oxime}}$ ), 980m ( $\text{N-O}_{\text{oxime}}$ ), 495m ( $\text{M-N}$ ), 440m ( $\text{M-O}$ ). Elemental anal. (%) calcd. For  $\text{C}_{30}\text{H}_{20}\text{N}_4\text{CuO}_2$ : C 67.72, H 3.79, N 10.53; Found: C 67.64, H 3.56, N 10.34. Zinc(II) complex was obtained as a light-yellow powder. Yield 72%, m.p. 175–177°C. IR (KBr) spectrum,  $\nu/\text{cm}^{-1}$ : 3055w ( $\text{C-H}_{\text{arom}}$ ), 1615s ( $\text{C=N}_{\text{imine}}$ ), 1590s ( $\text{C=N}_{\text{oxime}}$ ), 985s ( $\text{N-O}_{\text{oxime}}$ ), 510w ( $\text{M-N}$ ), 460w ( $\text{M-O}$ ).  $^1\text{H}$  NMR spectrum,  $\delta$ , ppm: 8.70 s (2H,  $\text{HC=N}_{\text{oxime}}$ ), 8.20–7.55 m (18H,  $\text{C-H}_{\text{arom}}$ ). Elemental anal. (%) calcd. For  $\text{C}_{30}\text{H}_{20}\text{N}_4\text{ZnO}_2$ : C 67.49, H 3.78, N 10.49; Found: C 67.33, H 3.67, N 10.38



**Scheme 2.** Synthesis of metal(II) complexes

### 3. Results and Discussion

The Schiff base ligand is soluble in ethanol, methanol, dichloromethane and diethyl ether. The metal complexes are soluble in dimethylformamide and dimethylsulfoxide and are insoluble in ethanol, acetone and chloroform. The elemental analysis values of the Schiff base ligand and complexes are compatible with those computed from the empirical formulas for every compound.

#### 3.1. FT-IR spectra

The FT-IR spectrum of the Schiff base ligand displayed peaks in the 3260, 990 and 3090  $\text{cm}^{-1}$  regions due to the constitution of ( $\text{O-H}_{\text{oxime}}$ ), ( $\text{N-O}_{\text{oxime}}$ ) and  $\text{C-H}_{\text{arom}}$  bonds. The bands in the 1645-1620  $\text{cm}^{-1}$  region are attributed to the ( $\text{C=N}_{\text{imine}}$ ) and ( $\text{C=NO}_{\text{oxime}}$ )

stretching frequencies. The spectrum of complexes showed characteristic ( $\text{-C=N}$ ) imine stretching vibrations at 1625–1615  $\text{cm}^{-1}$  and ( $\text{-C=N}$ ) oxime stretching vibrations at 1600-1590  $\text{cm}^{-1}$ . These frequencies showed that the imine and oxime bands were shifted to lower values by 20-30  $\text{cm}^{-1}$ . This important shift demonstrates a strong attachment of the metal centers to the imine-oxime chelating moieties. (Achiwawanich et al., 2014; Gondia and Sharma, 2018). The spectrum of the Ni(II), Cu(II), and Zn(II) complexes showed a new band at 510-470  $\text{cm}^{-1}$  of the ( $\text{M-O}$ ) bond resulting from the interaction between the oxime oxygen and the metal ions. The FTIR spectra of the metal and the imine nitrogen in the metal(II) complexes were supported by the appearance of new bands at 460-420  $\text{cm}^{-1}$  which were

assigned to (M–N). (El-Sherif and Eldebss, 2011; Al-Ne'aimi and Al-Khuder, 2013).

### 3.2. UV-Vis spectra and magnetic susceptibility

The UV-Vis spectra of the oxime-imine compounds were measured in  $10^{-3}$  M DMF solution at ambient temperature. The oxime-imine exhibited two absorption peaks around 265 and 340 nm. These peaks are ascribed to  $\pi \rightarrow \pi^*$  transitions, firstly being because of the aromatic ring and the secondly the imino group. The spectrum of the Cu(II) complex demonstrated a wide absorption band at 419 nm ( $\epsilon=648 \text{ mol}^{-1} \text{ L cm}^{-1}$ ) and 709 nm ( $\epsilon=406 \text{ mol}^{-1} \text{ L cm}^{-1}$ ) attributed to  ${}^2B_{1g} \rightarrow {}^2E_g$  and  ${}^2B_{1g} \rightarrow {}^2A_{1g}$  transition of a square-planar structure (El-Sherif and Eldebss, 2011; Vamsikrishna et al., 2016). The electronic spectrum of the Ni(II) complex indicated an absorption peak at 467 nm ( $\epsilon=968 \text{ mol}^{-1} \text{ L cm}^{-1}$ ) corresponds to the  ${}^3T_1(F) \rightarrow {}^3T_1(P)$  transition of a tetrahedral structure (Ali et al., 2015). The electronic spectrum of the Zn(II) complex showed an absorption peak at 423 nm ( $\epsilon=1367 \text{ mol}^{-1} \text{ L cm}^{-1}$ ) assignable the  $L \rightarrow M$  transition, which is harmonious by the complex having a tetrahedral geometry. (Gondia and Sharma, 2018). The magnetic moment value for copper chelate is 1.84 B.M., which shows a square-planar structure surround the copper ion. The value of nickel complex is 3.05 B.M. respectively, which demonstrate a tetrahedral structure surround the nickel(II) ion. The complex of zinc is diamagnetic as estimated for the  $d^{10}$  metal ion at a tetrahedral structure (Al-Ne'aimi and Al-Khuder, 2013).

### 3.3. ${}^1\text{H}$ NMR spectra

The  ${}^1\text{H}$  NMR spectrum is used to determine the structure of the synthesized ligand and its diamagnetic metal complexes. The  ${}^1\text{H}$  NMR

spectrum of the Schiff base ligand and its diamagnetic zinc(II) complex are presented in Figure 1. The  ${}^1\text{H}$  NMR spectrum of the ligand demonstrated a single peak at 9.15 ppm for the proton of the oxime group ( $=\text{N}-\text{OH}$ ). The signal that appeared at 9.15 ppm in the ligand has disappeared in the Zinc(II) complex, which confirms that the oxime group oxygen is involved in coordination with the metal. The  ${}^1\text{H}$  NMR spectrum of the ligand shows the oxime proton ( $\text{HC}=\text{N}$ ) resonance at 8.80 ppm, which shifts to 8.65 ppm in its zinc(II) complex, suggesting coordination by imine nitrogen and the oxime group oxygen. Further, the signals of the aromatic protons appeared the range of 8.50-7.75 ppm. These data are in good agreement with those previously reported for similar compounds. Since Ni(II) and Cu(II) complexes are paramagnetic; the  ${}^1\text{H}$  NMR spectra of the complexes could not be obtained. (Ifikhar et al., 2018; Ebrahimi et al., 2014).

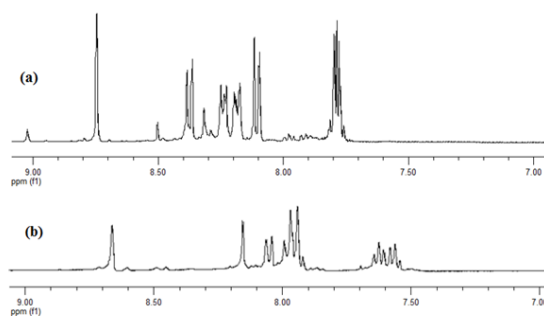


**Figure 1.**  ${}^1\text{H}$  NMR spectrum of Schiff base ligand and complex (a) Ligand (b) Zn(II) Complex

### 3.4. ${}^{13}\text{C}$ NMR spectra

The  ${}^{13}\text{C}$  NMR spectrum of the Schiff base ligand is given in Figure 2. In the  ${}^{13}\text{C}$  NMR spectrum of the ligand, the signals at 189.47 and 170.89 ppm are attributed to the carbon atoms of the imine group, and the carbon atoms of the oxime group. All the signals in the 148.80-126.20 ppm range are assigned to

the carbon atoms of the aromatic rings. The  $^{13}\text{C}$  NMR spectrums confirms the proposed structure of the Schiff base ligand (Uçan and Mercimek, 2005).

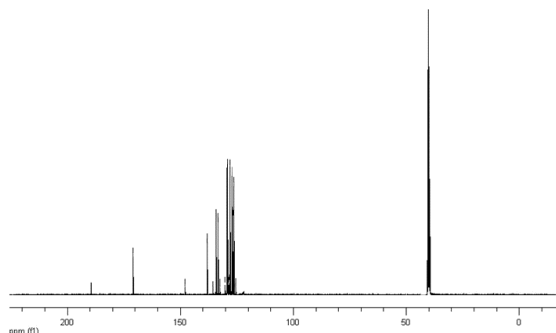


**Figure 2.**  $^{13}\text{C}$  NMR spectrum of ligand

### 3.5. Thermal Analysis

Thermogravimetric analysis of the complexes was studied starting from room temperature to  $900^\circ\text{C}$  at a heating rate of  $10^\circ\text{C}/\text{min}$  under  $\text{N}_2$  atmosphere (Figure 3). The weight loss was calculated at different temperatures and the range of the decomposition stages is given in Table 1. The TGA curve of the nickel(II) complex showed two steps of decomposition. The first stage in the temperature range from  $30\text{--}500^\circ\text{C}$  corresponds to the loss of  $\text{C}_{13}\text{H}_{13}\text{N}_2$  with approximated weight loss of  $37.70\%$ . The second stage was monitored in the range  $500\text{--}900^\circ\text{C}$  with mass loss of  $48.11\%$ , which was assigned to the partial decomposition of  $\text{C}_{17}\text{H}_7\text{N}_2\text{O}$ . Finally, the residual mass  $14.19\%$  corresponds well with its being  $\text{NiO}$  (Barfeie et al., 2018).  $\text{Cu(II)}$  complex decomposed in two essential step. The first stage was observed in the range  $30\text{--}400^\circ\text{C}$  with a mass loss of  $36.59\%$ , which is assigned to the partial decomposition of the  $\text{C}_{13}\text{H}_{10}\text{N}_2$ . The second decomposition step which commences at  $400^\circ\text{C}$  and terminates at

$900^\circ\text{C}$ , demonstrates a large mass loss of  $48.46\%$  assigned to the decomposition of  $\text{C}_{17}\text{H}_{10}\text{N}_2\text{O}$ . The final residual product of the  $\text{Cu(II)}$  complex is  $\text{CuO}$  (Chetana et al., 2016). The Thermogram of  $\text{Zn(II)}$  complex showed two decomposition stages. The first decomposition step of the zinc(II) complex occurs at the  $30\text{--}550^\circ\text{C}$  range. This step showed a weight loss of  $48.84\%$  which corresponds to the loss of  $\text{C}_{17}\text{H}_{12}\text{N}_2\text{O}$ . The second stage was observed in the range of  $550\text{--}650^\circ\text{C}$ , with a mass loss of  $35.88\%$ , which is due to the removal of  $\text{C}_{13}\text{H}_8\text{N}_2$ . The final thermal product at  $900^\circ\text{C}$  was zinc oxide (Rudbari et al., 2016; Uçan, 2019).

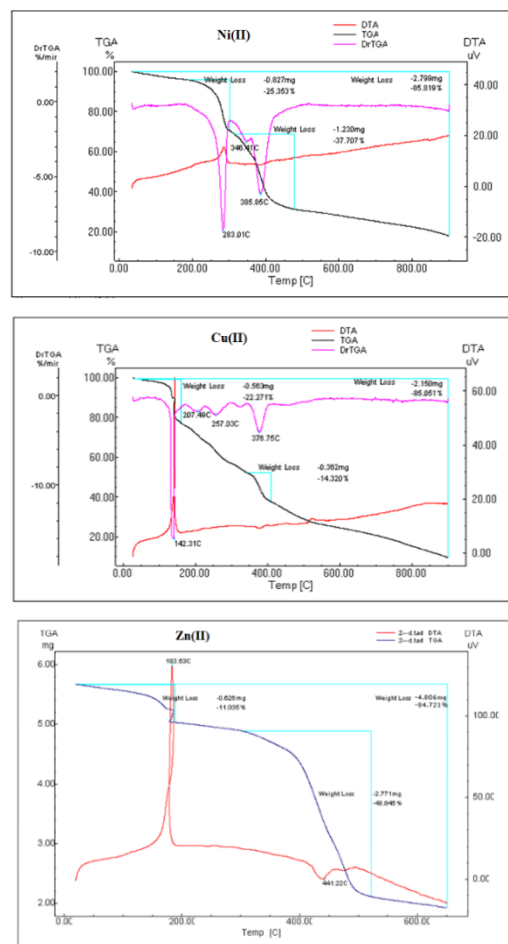


**Figure 3.** TGA and DTA curves of metal complexes



**Table 1.** Thermal degradation of the metal complexes

Compounds	M <sub>r</sub>	T (°C)	Weight loss % Found(Calcd.)	Assignment	Metallic residue % Found(Calcd.)
C <sub>30</sub> H <sub>20</sub> N <sub>4</sub> NiO <sub>2</sub>	527.20	30-500	37.70 (37.42)	C <sub>13</sub> H <sub>13</sub> N <sub>2</sub>	NiO
		500-900	48.11 (48.42)	C <sub>17</sub> H <sub>7</sub> N <sub>2</sub> O	14.19 (14.18)
C <sub>30</sub> H <sub>20</sub> N <sub>4</sub> CuO <sub>2</sub>	532.06	30-400	36.59 (36.51)	C <sub>13</sub> H <sub>10</sub> N <sub>2</sub>	CuO
		400-900	48.46 (48.54)	C <sub>17</sub> H <sub>10</sub> N <sub>2</sub> O	14.95 (14.94)
C <sub>30</sub> H <sub>20</sub> N <sub>4</sub> ZnO <sub>2</sub>	533.90	30-500	48.84 (48.75)	C <sub>17</sub> H <sub>12</sub> N <sub>2</sub> O	ZnO
		500-900	35.88 (36.00)	C <sub>13</sub> H <sub>8</sub> N <sub>2</sub>	15.26 (15.24)

### 3.6 SEM analysis

SEM technique has been tapped to determine the morphology of the metal compounds. The SEM images of the complexes revealed distinct images as is shown in Figure 4. The Nickel (II) complex showed an ice grains structure while and Copper(II) complexes gave regular size ice piece shaped structures. The SEM image of the Zinc(II) complex has looked like a crushed ice pieces. These complexes had typical different surface images (Barfeie et al., 2018; Kumar and Nath, 2019).

### 4. Conclusion

In summary, The results presented here gave good yields of the synthesised compounds. Analytical and spectral data of Cu(II) complex have put forward a square-planar structure surrounding the central metal ion. The Ni(II) and Zn(II) complexes have tetrahedral structure, respectively. The essential infrared spectral peaks of the complexes were compared with those of the oxime-imine. The weight losses for each complex were determined at certain temperatures as it is shown in TGA and DTG plots .

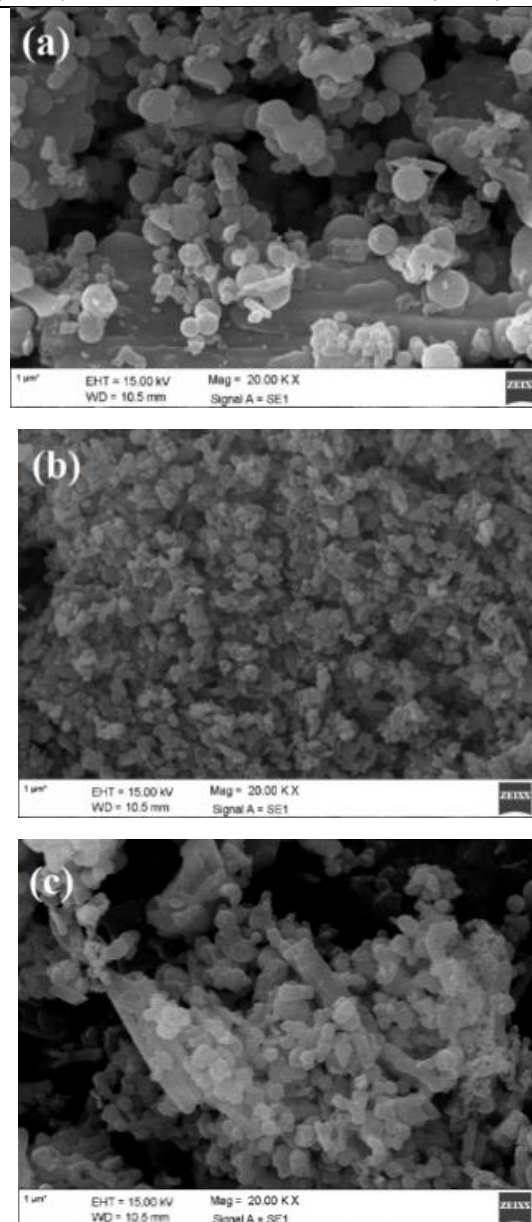


**Figure 4.** SEM morphologies of (a); Nickel(II), (b); Copper(II) and (c); Zinc(II) complexes

## 5. References

- Ali, O. A., El-Medani, S. M., Ahmed, D. A., & Nassar, D. A. (2015). Synthesis, characterization, fluorescence and catalytic activity of some new complexes of unsymmetrical Schiff base of 2-pyridine-carboxaldehyde with 2,6-diaminopyridine. *Spectrochimica Acta Part A: Molecular and Biomolecular Spectroscopy*, 144, 99-106.
- Al-Ne'aimi, M. M., & Al-Khuder, M. M. (2013). Synthesis, characterization and extraction studies of some metal(II) complexes containing (hydrazoneoxime and bis-acylhydrazone) moieties. *Spectrochimica Acta Part A: Molecular and Biomolecular Spectroscopy*, 105, 365-373.
- Al-Wabli, R. I., Govindarajan, M., Almutairi, M. S., & Attia, M. I. (2018). Spectral characterization, computed frequencies analysis and electronic structure calculations on (1E) N-hydroxy-3-(1H-imidazol-1-yl)-1-phenylpropan-1-imine: An oxime-bearing precursor to potential antifungal agents. *Journal of Molecular Structure*, 1168, 264-279.
- Barfeie, H., Grivani, G., Eigner, V., Dusek, M., & Khalaji, A. D. (2018). Copper (II), nickel(II), zinc(II) and vanadium(IV) Schiff base complexes: Synthesis, characterization, crystal structure determination, and thermal studies. *Polyhedron*, 146, 19-25.
- Chakravorty, A. (1974). Structural chemistry of transition metal complexes of oximes. *Coordination Chemistry Reviews*, 13(1), 1-46.
- Chetana, P. R., Srinatha, B. S., Somashekar, M. N., & Policegoudra, R. S. (2016). Synthesis, spectroscopic characterization, thermal analysis, DNA interaction and antibacterial activity of copper (I) complexes with N, N'-disubstituted thiourea. *Journal of Molecular Structure*, 1106, 352-365.
- Dede, B., Karipcin, F., & Cengiz, M. (2007). Novel Schiff bases with oxime groups and their homo-and heteronuclear copper (II) complexes. *Collection of Czechoslovak Chemical Communications*, 72(10), 1383-1397.
- Dede, B., Özen, N., & Görgülü, G. (2018). Synthesis, characterization, theoretical calculations and enzymatic activities of novel diimine-dioxime ligand and its homodinuclear Cu(II) complex. *Journal of Molecular Structure*, 1163, 357-367.
- Ebrahimi, H. P., Hadi, J. S., Abdalnabi, Z. A., & Bolandnazar, Z. (2014). Spectroscopic, thermal analysis and DFT computational studies of salen-type Schiff base complexes. *Spectrochimica Acta Part A: Molecular and Biomolecular Spectroscopy*, 117, 485-492.
- El-Sherif, A. A., & Eldebbs, T. M. (2011). Synthesis, spectral characterization, solution equilibria, in vitro antibacterial and cytotoxic activities of Cu(II), Ni(II), Mn(II), Co(II) and Zn(II) complexes with Schiff base derived from 5-bromosalicylaldehyde and 2-amino-methylthiophene. *Spectrochimica Acta Part A: Molecular and Biomolecular Spectroscopy*, 79(5), 1803-1814.
- Gondia, N. K., & Sharma, S. K. (2018). Spectroscopic characterization and photophysical properties of Schiff base metal complex. *Journal of Molecular Structure*, 1171, 619-625.
- Iftikhar, B., Javed, K., Khan, M. S. U., Akhter, Z., Mirza, B., & Mckee, V. (2018). Synthesis, characterization and biological assay of Salicylaldehyde Schiff base Cu(II)

- complexes and their precursors. *Journal of Molecular Structure*, 1155, 337-348.
- Kumar, L. V., & Nath, G. R. (2019). Synthesis, characterization and biological studies of cobalt(II), nickel(II), copper(II) and zinc (II) complexes of vanillin-4-methyl-4-phenyl-3-thiosemicarbazone. *Journal of Chemical Sciences*, 131(8), 76.
- Radha, V. P., Kirubavathy, S. J., & Chitra, S. (2018). Synthesis, characterization and biological investigations of novel Schiff base ligands containing imidazoline moiety and their Co(II) and Cu(II) complexes. *Journal of Molecular Structure*, 1165, 246-258.
- Rudbari, H. A., Iravani, M. R., Moazam, V., Askari, B., Khorshidifard, M., Habibi, N., & Bruno, G. (2016). Synthesis, characterization, X-ray crystal structures and antibacterial activities of Schiff base ligands derived from allylamine and their vanadium(IV), cobalt(III), nickel(II), copper(II), zinc(II) and palladium(II) complexes. *Journal of Molecular Structure*, 1125, 113-120.
- Singh, K., Barwa, M. S., & Tyagi, P. (2007). Synthesis and characterization of cobalt(II), nickel(II), copper(II) and zinc(II) complexes with Schiff base derived from 4-amino-3-mercaptop-6-methyl-5-oxo-1,2,4-triazine *European journal of medicinal Chemistry*, 42(3), 394-402.
- Tadavi, S. K., Yadav, A. A., & Bendre, R. S. (2018). Synthesis and characterization of a novel Schiff base of 1, 2-diaminopropane with substituted salicylaldehyde and its transition metal complexes: Single crystal structures and biological activities. *Journal of Molecular Structure*, 1152, 223-231.
- Tolga Colak, A., Irez, G., Mutlu, H., Hökelek, T., & Çaylak, N. (2009). A Co (III) complex with a tridentate amine-imine-oxime ligand from 1, 2, 3, 4-tetrahydroquinazoline: synthesis, crystal structure, spectroscopic and thermal characterization. *Journal of Coordination Chemistry*, 62(6), 1005-1014.
- Uçan, S. Y. (2019). Schiff Bazı Komplekslerinin Sentezi Ve Yapılarının İncelenmesi. *Niğde Ömer Halisdemir Üniversitesi Mühendislik Bilimleri Dergisi*, 8(1), 621-629.
- Uçan, S. Y. (2020). Synthesis and Spectroscopic Characterization of Bidentate Schiff Base and Zinc (II) Complex. *Eurasian Journal of Science Engineering and Technology*, 1(1), 35-40.
- Uçan, S. Y., & Mercimek, B. (2005). Synthesis and characterization of Tetradentate N<sub>2</sub>O<sub>2</sub> Schiff base ligands and their transition metal complexes. *Synthesis and Reactivity in Inorganic, Metal-Organic and Nano-Metal Chemistry*, 35(3), 197-201.
- Vamsikrishna, N., Kumar, M. P., Tejaswi, S., & Rambabu, A. (2016). DNA binding, cleavage and antibacterial activity of mono-nuclear Cu(II), Ni(II) and Co(II) complexes derived from novel benzothiazole Schiff bases. *Journal of fluorescence*, 26(4), 1317-1329.
- Yıldırım, S., İhsan Pekacar, A., & Uçan, M. (2003). The Synthesis of Four New bis (Amino- 2- naphthylglyoximes) and Their Polymeric Complexes. *Synthesis and reactivity in inorganic and metal-organic chemistry*, 33(7), 1253-1261.